Available at www.sciencedirect.com

ScienceDirect

journal homepage: www.elsevier.com/locate/he

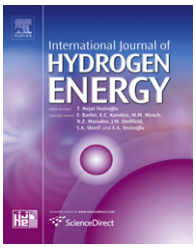

Solar hydrogen production by the Hybrid Sulfur process

*Claudio Corgnale, William A. Summers**

Savannah River National Laboratory, Aiken, SC 29808, USA

ARTICLE INFO

Article history:
Received 17 March 2011
Received in revised form
24 May 2011
Accepted 27 May 2011
Available online 5 August 2011

Keywords:
Hydrogen
Thermochemical
Hybrid Sulfur
Solar
Design
Cost

ABSTRACT

A conceptual design and economic analysis are presented for a hydrogen production plant based on the use of thermochemical water splitting combined with a solar central receiver. The reference design consists of a Hybrid Sulfur thermochemical process coupled to a solar plant, based on the particle receiver concept, for a yearly average hydrogen production rate of 100 tons per day. The Hybrid Sulfur plant has been designed on the basis of results obtained from a new flowsheet ASPEN Plus® simulation, carrying out specific evaluations for the Sulfur dioxide Depolarized Electrolyzer, being developed and constructed at Savannah River National Laboratory, and for the sulfuric acid decomposition bayonet-based reactor, investigated at Sandia National Laboratory. Solar hydrogen production costs have been estimated considering two different scenarios in the medium to long term period, assuming the financing and economic guidelines from DOE's H2A model and performing ad hoc detailed evaluations for unconventional equipment. A minimum hydrogen production specific cost of 3.19 $/kg (2005 US $) has been assessed for the long term period. The costs, so obtained, are strongly affected by some quantities, parameters and assumptions, influence of which has also been investigated and discussed.

1. Introduction

The push for lowering the consumption of fossil-based fuels, both for stationary power production and for vehicles, is dictated by a need for reducing the addiction to fossil fuels and for lowering emissions of pollutants, such as carbon dioxide, particulate, etc.

Widespread use of hydrogen as an energy carrier (and fuel) to replace liquid and gaseous fuels is one of the viable methods to accomplish it in the medium to long term period. Hydrogen can complement electricity as the major energy carriers in what has been referred to as the Hydrogen Economy. Electricity can be used to produce hydrogen from water; and hydrogen can be used to generate electricity using fuel cells. Hydrogen provides a means of energy storage, which is especially important as future energy systems employing a large percentage of renewable energy sources are considered. For example, renewable resources, such as solar energy or wind power, can be used to produce hydrogen, which can be transported and stored for later use in automobiles or other applications.

Although hydrogen is the most abundant element in the universe, it is very reactive and does not occur in significant quantities in a pure state on the Earth. Hydrogen is practically present only bound to other atoms (e.g. oxygen, carbon) to form molecules of various kind (e.g. water, hydrocarbons). Thus, to make the Hydrogen Economy a real possibility, an important issue to be addressed regards the hydrogen

* *Corresponding author*. Tel.: +1 803 725 7766; fax: +1 803 725 8829.
E-mail address: william.summers@srnl.doe.gov (W.A. Summers).
0360-3199/$ – see front matter
doi:10.1016/j.ijhydene.2011.05.173

Nomenclature

c_{pH}	Helium specific heat, J/kg-°C
c_{pS}	Sand specific heat, J/kg-°C
d_p	Sand particle mean diameter, m
D_T	IHX tube diameter, m
f	Corrective factor for LMTD
GA	General Atomics
H2A	Hydrogen Analysis (DOE code)
HHV	Higher Heating Value
HyS	Hybrid Sulfur cycle
IHX	Intermediate Heat Exchanger
INL	Idaho National Laboratory
LHV	Lower Heating Value
LMTD	Log Mean Temperature Difference in the IHX, °C
m_{He}	IHX loop helium flow rate, kg/s
Nu_H	IXH tube side (helium) Nusselt number, defined as: $U_H \cdot D_T/\lambda_H$
Nu_S	IXH shell side (sand) Nusselt number, defined as: $U_S \cdot D_T/\lambda_S$
O&M	Operating and maintenance
p	IHX loop helium maximum pressure, bar
PCF	Plant capacity factor
Pe_S	IXH shell side (sand) Peclet number, defined as: $v_S \cdot c_{pS} \cdot \rho_S \cdot D_T/\lambda_S$
Pr_H	IXH tube side (helium) Prandtl number, defined as: $c_{pH} \cdot \mu_H/\lambda_H$
Re_H	IXH tube side (helium) Reynolds number, defined as: $\rho_H \cdot v_H \cdot D_T/\mu_H$
S	Heat transfer area in the IHX, m^2
SDE	SO_2 depolarized electrolyzer
SI	Sulfur Iodine cycle
SNL	Sandia National Laboratory
SRNL	Savannah River National Laboratory
T_2	IHX loop station 2 temperature (Fig. 10), °C
T_3	IHX loop station 3 temperature (Fig. 10), °C
T_4	IHX loop station 4 temperature (Fig. 10), °C
T_5	IHX loop station 5 temperature (Fig. 10), °C
TPD	Tons per day
U_g	Overall heat transfer coefficient in the IHX, W/m^2-°C
U_H	IHX tube side (helium) heat transfer coefficient, W/m^2-°C
U_S	IHX shell side (sand) heat transfer coefficient, W/m^2-°C
v_H	IHX helium stream velocity, m/s
v_S	Approach velocity of sand stream, m/s
W	Thermal power exchanged in the IHX, W

Greek letters

β	IHX loop compression ratio
η	HyS process efficiency
η_c	IHX loop compressor overall efficiency (accounting for isentropic and mechanical efficiency)
η_{el}	Thermal-electric efficiency
λ_H	IHX helium conductivity, W/m-°C
λ_S	IHX sand conductivity, W/m-°C
μ_H	Helium viscosity, kg/m-s
μ_S	Sand viscosity, kg/m-s
ρ_H	Helium density, kg/m^3
ρ_S	Sand density, kg/m^3

production. Water splitting and biomass decomposition [1] seem to be the best methods to produce hydrogen globally avoiding CO_2 production.

To generate hydrogen by water molecule splitting, only electrolysis [2] and thermochemical processes [3,4] seem to have potential to be real candidate on both small and large scale scenarios. The first process requires external electric power, while thermochemical cycles require external thermal power and, depending on the cycle, also electric power. Since conventional (low temperature) electrolysis is based on using electricity to dissociate water, the overall hydrogen production efficiency is the product of the electric generating efficiency and the electrolyzer efficiency. The resultant overall efficiency is likely only 20–24%, based on the Lower Heating Value (LHV) of the product hydrogen. More efficient processes, including steam (high temperature) electrolysis and thermochemical cycles have been identified. Overall hydrogen generation efficiencies of over 40% may be possible, resulting in the production of nearly twice as much hydrogen for the same amount of energy input.

Thermochemical processes operate indirect water splitting by means of auxiliary substances, which are recycled inside the plant with a series of externally driven chemical reactions. In general, thermochemical cycles are more attractive than water electrolysis because of their higher efficiency [3–5]. Since 1960's more than 100 processes have been analyzed and deeply investigated to see the effective potential as candidates to produce H_2 [3,4,6]. Sulfur family thermochemical cycles, which see a common high temperature H_2SO_4 decomposition section, are among the most attractive ones, due to their favorable intrinsic features compared to other competitive processes (e.g. relatively low temperatures, low dangerousness of recycled substances, good knowledge of chemical reactions in the H_2SO_4 decomposition section, etc.) [3,4].

In particular the Hybrid Sulfur (HyS) cycle, which is being investigated all around the world, was identified by the Nuclear Hydrogen Initiative (NHI) program as one of the first priority baseline processes to be coupled to a nuclear plant, as well as it is among the main candidates for solar hydrogen production, within the DOE Solar Thermochemical Hydrogen (STCH) project.

Savannah River National Laboratory has been involved in developing and building the SO_2 depolarized electrolyzer (SDE), which is the distinguishing component of the HyS plant, inside the NHI program, and is involved in the STCH project to evaluate the effective techno-economic feasibility of the HyS plant driven by solar power. The latter activity results are the matter of the present paper.

2. The HyS process

The HyS cycle was first proposed by Westinghouse Electric Corporation and developed since 1970s and 1980s [7–10].

This cycle is one of the most advanced, promising and simplest thermochemical processes, comprising only two global reaction steps and having only fluid reactants.

A simple scheme of the process is reported in Fig. 1.

The first step (sulfuric acid decomposition section) where H_2SO_4 is decomposed into SO_2, O_2 and H_2O is common to all sulfur-based thermochemical cycles. This is an endothermic process which requires external power to be delivered at temperatures usually higher than 800 °C to make the decomposition feasible. Depending on features of the overall process, H_2SO_4 (in a water mixture) needs to be preliminarily concentrated and vaporized. Upon further heating it decomposes, producing sulfur trioxide (SO_3) and steam (de-hydration reaction):

$$H_2SO_4(aq) \rightarrow SO_3(g) + H_2O(g) \quad (1)$$

After further heating in a catalytic reactor, SO_3 is split into SO_2 and O_2:

$$SO_3(g) \rightarrow SO_2(g) + 1/2O_2(g) \quad (2)$$

The mixture of SO_3, SO_2, O_2, H_2O and un-reacted H_2SO_4 decomposition, is cooled and, after O_2 is removed from the process, SO_2 and H_2O are recycled and suitably combined again, feeding the anode of the SDE (Fig. 2), which is the essential component of the second step (SO_2 oxidation section) of the HyS cycle.

Sulfur dioxide is electrochemically oxidized at the anode of the SDE to form H_2SO_4, protons and electrons (Fig. 2), following the reaction (3):

$$SO_2 + 2H_2O \rightarrow H_2SO_4 + 2H^+ + 2e^- \quad (3)$$

Protons H^+ are conducted across the electrolyte separator to the cathode and recombine with electrons e^- (forced to pass through an external circuit) to form H_2.

$$2H^+ + 2e^- \rightarrow H_2 \quad (4)$$

The H_2SO_4 produced at the anode is recycled to the H_2SO_4 decomposition section, closing the cycle (Fig. 1).

The standard cell potential for SO_2 depolarized electrolysis is −0.158 V at 25 °C [5], while the reversible potential for SO_2 dissolved to saturation at 1 bar in a 50 wt.% H_2SO_4–H_2O solution becomes −0.243 V [5]. This implies that the HyS cycle electricity consumption is much lower than water electrolysis process, being the reversible potential for water electrolysis at

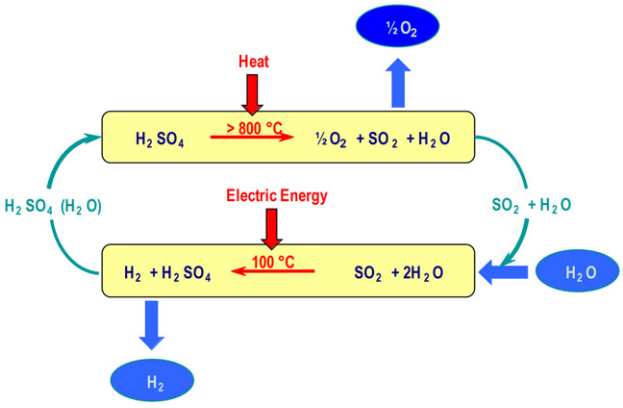

Fig. 1 – The HyS cycle scheme.

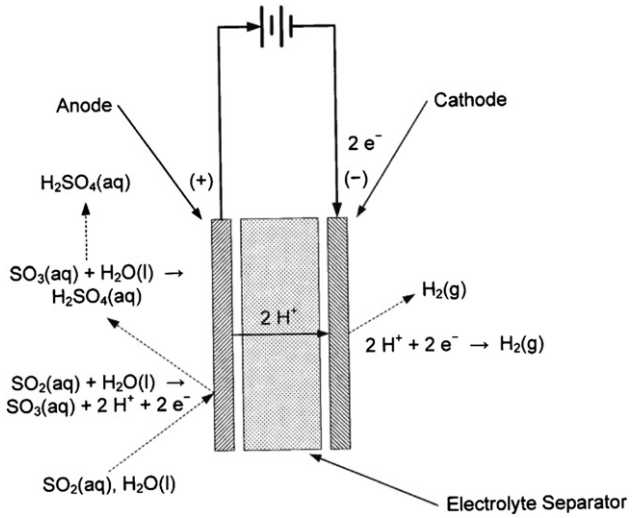

Fig. 2 – The SO_2 Depolarized Electrolyzer (SDE) concept.

25 °C equal to −1.229 V [5]. Actually, the SDE is expected to operate at potential higher than −0.243 V, mainly due to ohmic resistance losses, mass transport losses and kinetic resistance losses[1]. On the basis of experimental results obtained at SRNL, a potential of −0.6 V is attainable at current density of 500 mA/cm^2, under operating temperatures of the order of 100 °C, pressures of greater than 10 bar and with an anode feed stream consisting of SO_2 dissolved in a 50 wt% H_2SO_4–H_2O solution. Under these conditions, with a working pressure of 21 bar, the SDE requires 115.7 kJe/molSO_2. This represents the goal for the SRNL's SDE and the baseline conditions for further evaluations carried out in the remainder of the paper. More details regarding the activities carried out on the SDE are reported elsewhere [5].

The other essential component of the HyS process is the high temperature H_2SO_4 decomposition reactor. An innovative bayonet heat exchanger-based reactor has been assumed as the baseline concept, since it is particularly adequate to meet the requirements of the sulfuric acid decomposition process in the HyS plant. In particular, by this approach: (1) the high temperature internal heat recovery is realized in a single heat exchange device; (2) all the external connections can be made at relatively low temperatures, allowing the use of polytetrafluoroethylene of similar (inexpensive) materials for seals.

A simplified schematic of this device is depicted in Fig. 3. The concentrated liquid H_2SO_4 water mixture, which feeds the bayonet reactor (Inlet in Fig. 3), is boiled, dehydrated, superheated and catalytically decomposed into SO_2, O_2 and H_2O, in the outer annular zone of the device. The high temperature product goes down through the inner tubular part of the bayonet, where water condenses and SO_3 and H_2O recombine into H_2SO_4, releasing heat to the feeding mixture. Further heat amount is supplied by a high temperature external source, to make the overall decomposition process feasible.

Silicon carbide (SiC) material seems to be able to resist such extreme conditions (i.e. high temperatures, corrosive and oxidizing environments, etc.) and shows excellent heat

[1] Water electrolysis is expected to operate at voltage levels higher −1.229 V, in the range of −1.8 V to −2.0 V.

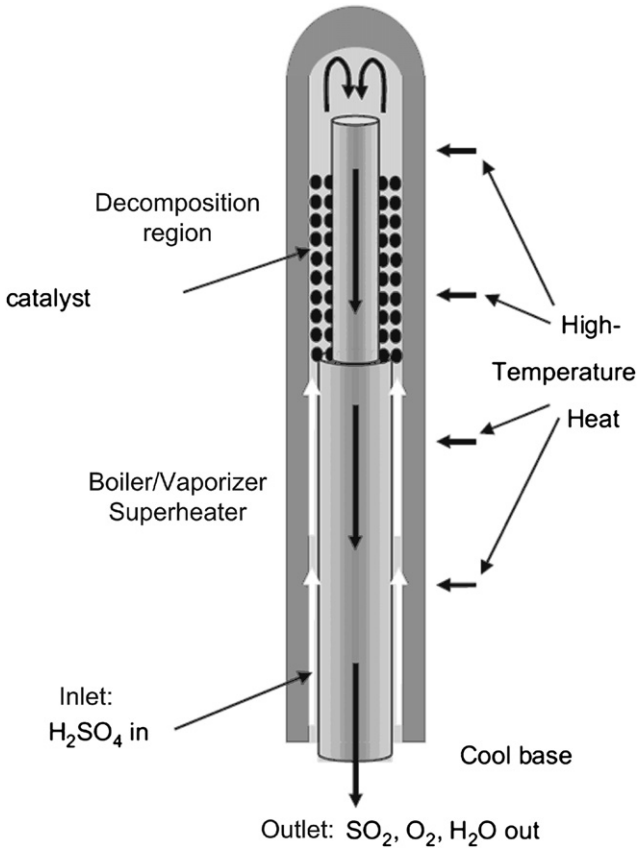

Fig. 3 – Schematic of the bayonet-based H_2SO_4 decomposer.

transfer features (i.e. high conductivity). The baseline bayonet reactor was developed at Sandia National Laboratory (SNL), which has been the leading investigator in the decomposition of sulfuric acid for the NHI program. The design utilizes SiC as the constitutive tube materials, both for the external end-closed tube and for the internal open tube. These SiC shapes are easily (and already) available. A prototype reactor was built and successfully demonstrated by SNL under the NHI program [11].

A numerical model of the bayonet reactor has been set up at SRNL basically considering a lumped parameter steady state plug flow reactor concept, constituted by more than 100 single reactor units, and taking into account chemical equilibrium reactions. A more detailed description, with all the assumptions, can be found elsewhere [5].

Steady state simulations of the bayonet model have been carried out by ASPEN Plus® in order to find the minimum external power requirement for the H_2SO_4 decomposition process, under different operating conditions.

On the basis of results obtained from the simulations and considerations on the solar matching of the HyS plant, carried out at SRNL, the solar coupled bayonet reactor has been assumed to work under the following conditions: (1) the feed H_2SO_4 water mixture concentration is 75 wt.%, (2) the pressure of the feeding H_2SO_4 mixture is 40 bar, (3) the peak temperature is 920 °C. An overall pressure drop of 2 bar inside the bayonet has also been assumed, on the basis of evaluations carried out at SRNL.

ASPEN Plus® simulation results for the solar case are reported in Fig. 4.

The concentrated H_2SO_4 mixture feeds the component at 40 bar and 120 °C and it is preheated, vaporized and superheated up to 675 °C with first decomposition process of H_2SO_4 into SO_3. This temperature has been set as the catalytic decomposition starting temperature. H_2SO_4 (and SO_3) is catalytically decomposed into SO_2 and O_2 up to 920 °C in gaseous phase and the product is cooled to 480 °C, with re-association of SO_3 and water into H_2SO_4, and condensed down to temperatures of the order of 256 °C.

In Fig. 5 H_2SO_4 decomposer heating and cooling curves obtained by pinch analysis of the bayonet model are reported

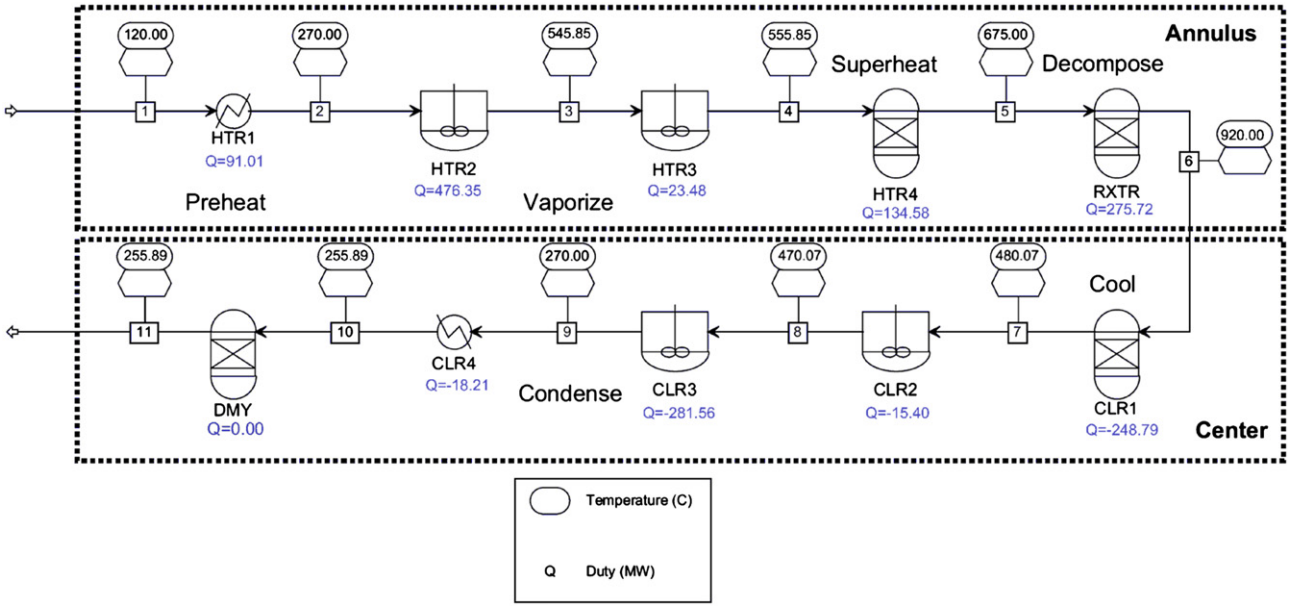

Fig. 4 – ASPEN Plus® bayonet model with results for a feed flow rate of 275.6 kg/s (with production of 1.39 kmol/s of SO_2) under solar case operating conditions (feed H_2SO_4 mixture 75 wt.%, inlet pressure 40 bar, peak temperature 920 °C) with pressure drop of 2 bar.

plotting the temperatures in the ordinate and the relative heat duty in the abscissa, under the solar case conditions, assuming a pinch of 10 °C. A minimum high temperature heat duty (hot utility) of 358 kJ/molH_2 is required with the pinch temperature at approximately 363 °C (373 °C in the cooling curve). A cold utility duty of approximately 109 kJ/molH_2 is needed to lower the product stream temperature from 256 °C to 120 °C.

Based on the pinch analysis, the grand composite curve has been constructed for a feeding flow rate of 275.6 kg/s. This profile is reported in Fig. 6, showing that the needed external power can be delivered by a hot utility fluid, such as helium, air, etc, at temperature of 950 °C down to 400 °C, assuming a minimum temperature difference of 25 °C for the integrated heat transfer process. The profile shown in Fig. 6 represents the solar baseline approach to deliver the needed thermal power to the H_2SO_4 decomposition process.

On the basis of solar case boundary conditions, considerations and results obtained for the SDE and the bayonet reactor a new detailed flowsheet has been developed at SRNL, initially set up for a nuclear driven HyS cycle [5] and then suitably adapted to the present solar case (Fig. 7) considering different working conditions.

This flowsheet has been developed with the aim of achieving the best integration between the SDE and the bayonet decomposer and the highest allowable efficiency, considering only commercially available equipment, for the more traditional components of the cycle, adequately modified and designed for the specific operating conditions of the various plant sections. With reference to Fig. 7, SO_2 is dissolved in 43wt.% sulfuric acid and fed to the anode of the SDE (Stream 2). Approximately 40% of the SO_2 is reacted, producing H_2SO_4 in water at 50 wt.% leaving the SDE (Stream 11). This solution seems to represent the best compromise between electricity consumption and SO_2 recycling inside the process (i.e. to reach the highest efficiency).

The H_2SO_4–SO_2 water mixture produced at the SDE anode is then concentrated up to 75 wt.% before feeding the decomposition reactor. The concentration of H_2SO_4 is realized by two flashes in series, KO-02 and KO-03, (operating at 1 and 0.3 bar) and a vacuum column, TO-01, (at 0.13 bar) which requires low temperature thermal power for the reboiler. The SO_2 extracted from the H_2SO_4 concentration section is recycled (SO_2 Recycle Compressor) and sent to the Anolyte Prep Tank, feeding the anode of the SDE. The H_2SO_4 undecomposed in the high temperature reactor is recycled and concentrated again (KO-06, KO-07 and TO-01).

The O_2 produced in the sulfuric acid decomposer needs separating from SO_2 and H_2O before extraction as byproduct. The O_2 separation is realized by 4 knock out devices (KO-08, KO-09, KO-10, KO-11) operating at different pressures and by an absorber-column (TO-02).

Energy balances of the process are reported in Table 1, based upon ASPEN Plus® simulation results.

The high temperature power delivered to the bayonet decomposer represents almost 83% of the overall thermal power needed to sustain the HyS process. The remainder is needed to the H_2SO_4 concentration column boiler. Approximately 97% of the electric power is needed for the SDE and the remainder is due to auxiliary equipment inside the HyS process (i.e. compressor and pumps). Hydrogen is produced at 100 °C and 21 bar.

The HyS process efficiency, η, is defined as follows:

$$\eta = \frac{\text{Out } H_2 \text{ Thermal Power}}{\text{High } T \text{ Thermal Power} + \text{Low } T \text{ Thermal Power} + \dfrac{\text{Electric Power}}{\eta_{el}}} \quad (5)$$

with out H_2 Thermal Power (MWt) being the thermal power available from the hydrogen produced in the plant and based on the H_2 LHV; High T Thermal Power (MWt) the needed thermal power supplied to the process to decompose H_2SO_4; Low T Thermal Power (MWt) the needed thermal power to concentrate sulfuric acid and Electric Power (MWe) the electric power supplied to the HyS process for the SDE and auxiliaries, with a thermal-electric efficiency, η_{el}.

The current HyS process, based on the commercial flowsheet described above, shows an efficiency of approximately 33%, based upon the LHV of hydrogen and assuming η_{el} equal to 40%. This is equivalent to a hydrogen production efficiency of 39% based on the Higher Heating Value (HHV), a method more commonly used in the electric power industry. Advances to the HyS process have been identified that could raise the efficiency to 40% (LHV) or 48% (HHV) in the future.

3. The solar-thermochemical plant matching

Due to the maximum temperatures usually achieved in the HyS cycle, the particle (sand) receiver solar tower concept has been selected to collect the needed solar thermal energy and deliver it to the thermochemical process.

A schematic of the solar tower is shown in Fig. 8 along with the HyS plant interfaced equipment and the IHX loop, which transfers heat from solar hot particle (sand) to HyS interfaced components working fluid by means of an intermediate thermal carrier. As shown in the figures, both the bayonet reactor and the H_2SO_4 concentration column boiler have been assumed to be fed by the same solar tower[2].

[2] To supply low temperature heat to the column reboiler different approaches have been investigated: (1) steam heat pump, recovering the heat available from the column condenser; (2) solar condensing steam turbine power plant; (3) solar steam back pressure turbine power plant. Based on results achieved and to have a more simplicity in the arrangement [22], presently, both the high temperature thermal power and low temperature thermal power have been assumed supplied by the same solar source.

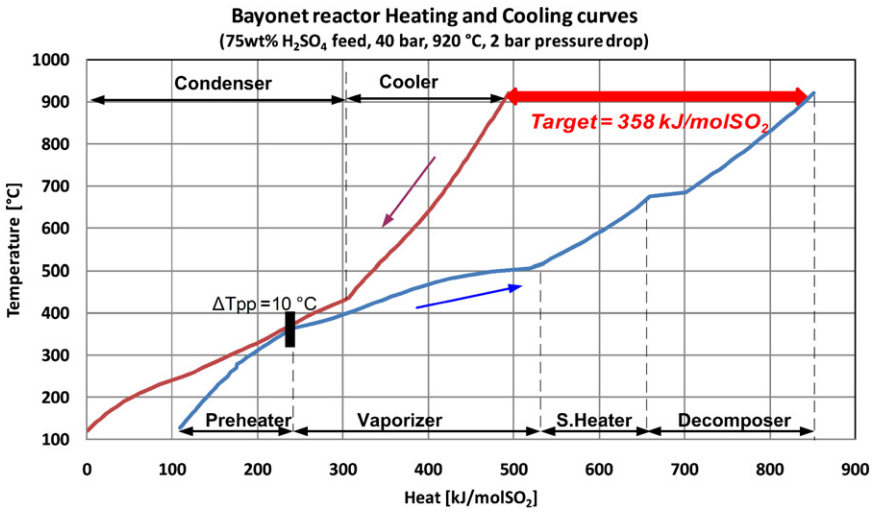

Fig. 5 – Bayonet reactor pinch analysis composite curves (temperature vs heat duty) under the solar case operating conditions (feed H_2SO_4 mixture 75 wt.%, inlet pressure 40 bar, peak temperature 920 °C) with pressure drop of 2 bar.

Alumina particle sand (with an average size of 600 μm) is heated up to 1000 °C absorbing solar radiation inside the insulated open cavity sand receiver. The particle receiver concept is studied and developed at SNL [12–14] and a scheme is reported in Fig. 9. Particles fall as a thin curtain close to the rear walls of the receiver, so they absorb thermal power from the direct solar insolation that passes through the receiver aperture and from the heater walls of the cavity. The heated particles are then stored in the hot sand storage tank at temperature of 1000 °C. A controlled flow of sand is permitted to pass across the IHX from temperature of 1000 °C (T_3 in Fig. 10) to temperature of 600 °C (T_4 in Fig. 10). An intermediate heat transfer fluid, such as helium or air, is heated in the IHX and, in turn, delivers to the HyS plant both high temperature thermal power for the bayonet reactor and low temperature thermal power for the column reboiler. Sand is then stored in the cold sand storage tank at 600 °C. The use of an intermediate heat transfer fluid to carry heat between the IHX and the bayonet reactor was chosen to increase reliability and to simplify the design of these units. However, it was considered that the direct heating of the bayonet by the falling sand was feasible following further development. This was considered in the long term solar plant design.

Cold particles are extracted from the cold sand storage tank and transported to the top of the receiver by a ceramic-lined mechanical bucket lift, and stored in a buffer storage area. The primary purpose is to alleviate the mismatch between the potentially rapid variation in particle mass flow rates through the receiver and the relatively slow response time of the lift system. The particle mass flow rate extracted from the buffer storage system, entering the receiver cavity, is controlled by a regulating feeder.

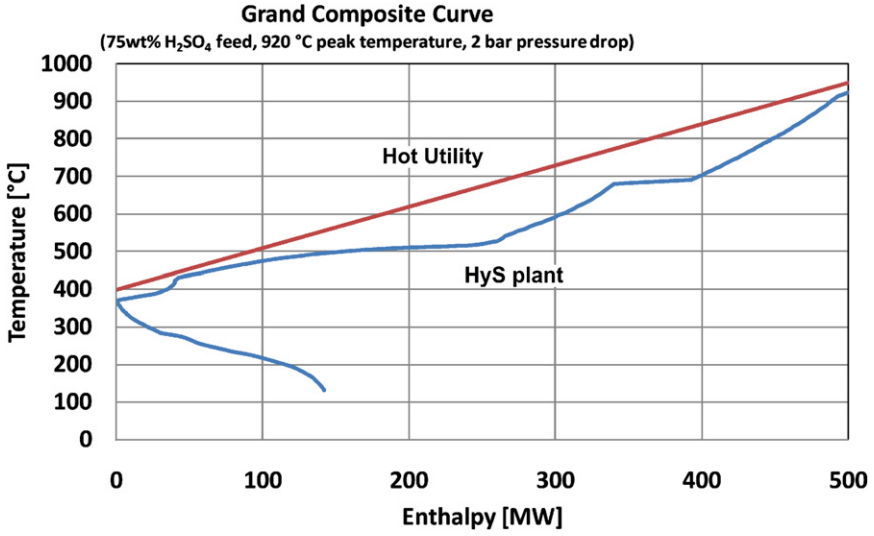

Fig. 6 – Bayonet reactor pinch analysis grand composite curve under the solar case conditions (feed H_2SO_4 mixture 75 wt.%, inlet pressure 40 bar, peak temperature 920 °C) with pressure drop of 2 bar, for a feed flow rate of 275.6 kg/s with a production of 1.39 kmol/s SO_2.

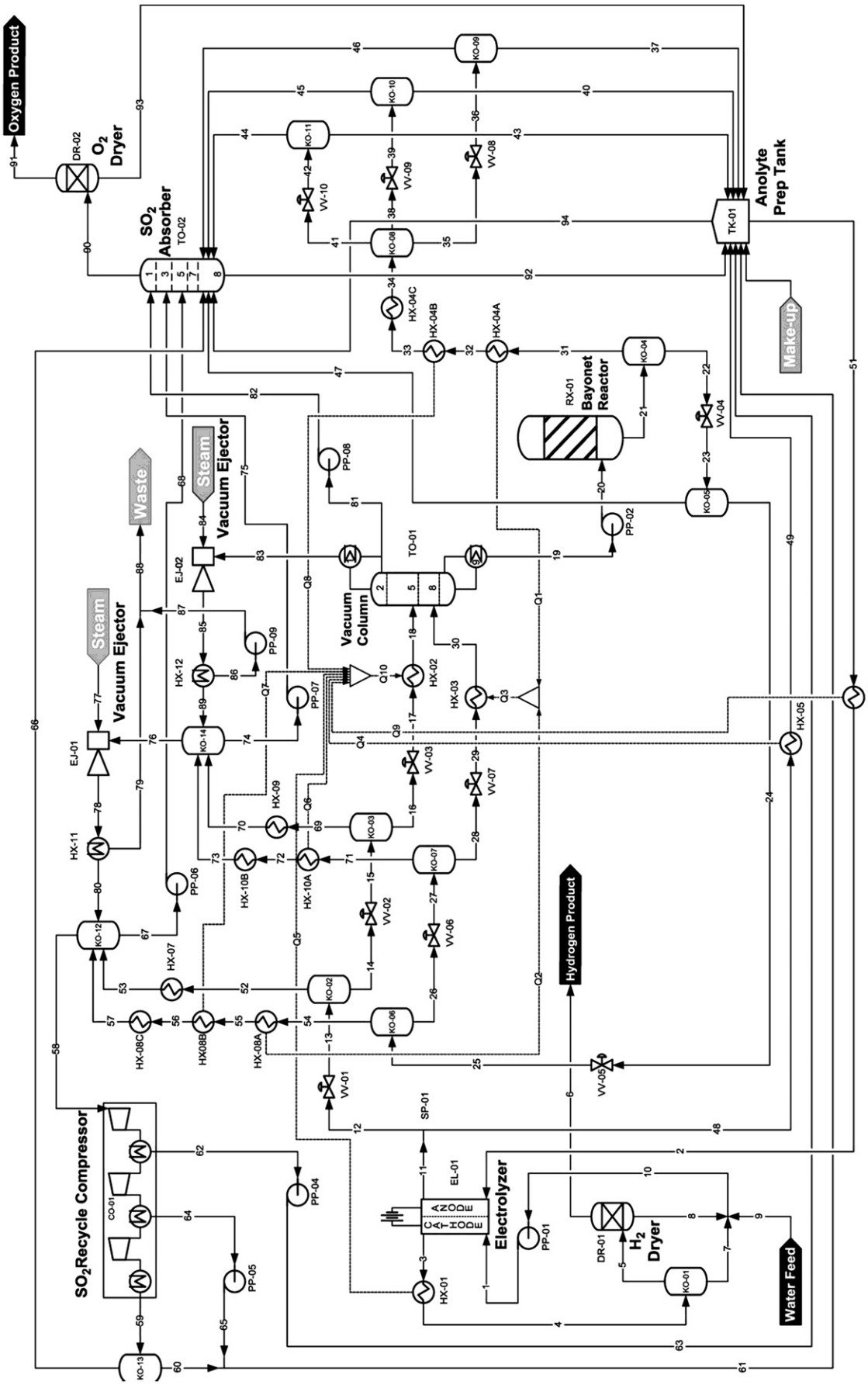

Fig. 7 – HyS cycle flowsheet.

Table 1 – Net specific (per molH_2) energy balance of the HyS cycle.

Output	*Power* [kJ/molH_2]
H_2 production	242.0 (LHV based)
Input	*Power* [kJ/molH_2]
High temperature thermal power (H_2SO_4 decomposition)	358.0
Low temperature thermal power (H_2SO_4 concentration column boiler)	75.5
Electric power (Electrolyzer and auxiliaries)	119.5

Sand thermal storage equipment is needed to compensate for the discontinuous and variable solar insolation during the day and throughout the year. By this approach the IHX is allowed to operate continuously, assuring working continuity throughout the year for the overall HyS chemical process.

The IHX loop schematic flowsheet is shown in Fig. 10.

The present configuration sees helium as the IHX loop energy carrier due to its inertness, good heat transfer characteristics and potential leverages from nuclear applications. The IHX loop can be modeled by classical heat exchange process relationships (i.e. mass and energy balances). Equation system, so obtained, can be solved once values of a set of quantities are known or established. These quantities are: p, β, η_c, T_2, T_5, m_{He}.

For the present IHX loop p value has been set to 40 bar β value has been assumed equal to 1.034, with pressure drops of the order of 1.3 bar for the overall IHX circuit and η_c has been assumed equal to 0.73 (isentropic efficiency equal to 0.75 and mechanical efficiency approximately equal to 0.975 which

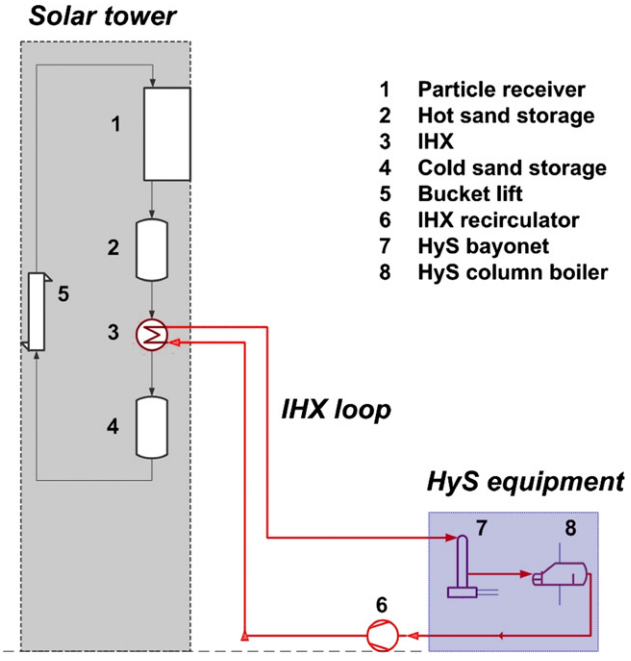

Fig. 8 – The solar plant concept: the solar tower receiver is matched to the HyS plant interfaced equipment by an intermediate heat transfer loop (IHX loop).

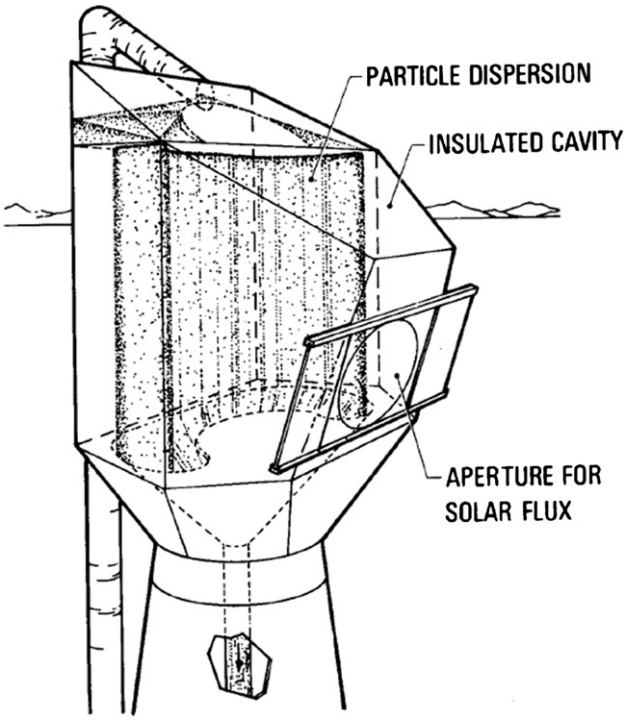

Fig. 9 – Conceptual design of particle solar receiver (from SNL).

are reasonable values for a massive H_2 production). A pinch temperature difference of 50 °C has been imposed for the IHX on the basis of typical values for nuclear applications. Thus T_2 is equal to 950 °C. According to evaluations carried out for the bayonet reactor, considering that the lower T_5, the lower recirculation compression work is, T_5 has been fixed equal to 400 °C. Once m_{He} is known, which value is a function of the H_2 production level, the IHX loop flowsheet stream quantities can be determined unequivocally.

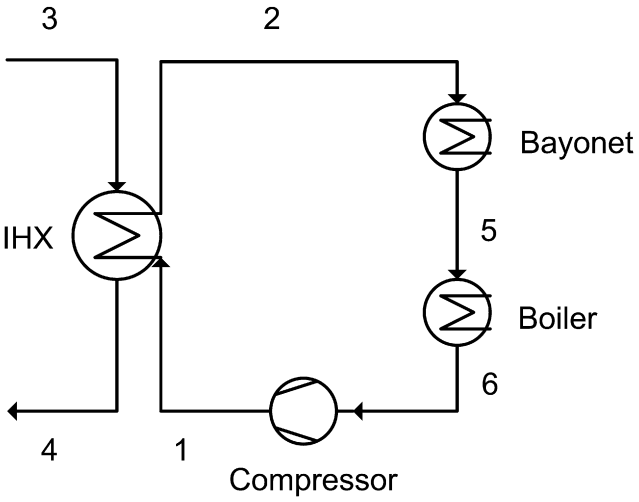

Fig. 10 – Intermediate heat exchanger loop (IHX loop): heat is transferred from sand (3–4) to heat carrier (1–2) and, in turn, delivered to the HyS equipment (Bayonet reactor: 2–5 and Column boiler: 5–6). A compressor (6–1) is needed to re-circulate heat carrier fluid.

Further evaluations are being carried out at SRNL to assess the best operating pressure value, which comes out from the optimum design point considering investment costs, lifetime costs and system reliability.

4. The HyS solar plant energy balance

The U.S. Department of Energy has created a hydrogen analysis tool (H2A) [15] that provides a standard format and list of parameters for reporting analysis results for various hydrogen processes, including centralized production. The DOE's H2A guidelines have been assumed as the baseline approach to carry out the design and economic evaluations of the solar H_2 production system, considering two different time scenarios to evaluate the performance and economic potential of the solar HyS plant in the medium to long term period. The first scenario sees 2015 as the starting year, while the second scenario, for a longer period, sees the starting year at 2025.

The solar HyS plant has been designed assuming a yearly average hydrogen production level of 100 metric tonnes per day (TPD), or 578 mol/s. Given the Southwest USA desert insolation features and weather, based on calculations carried out by SNL, a plant capacity factor (PCF) of 75% (76% for the 2025 year) can be practically achieved, with a maximum solar thermal storage of 13 h during the summer solstice (design point) and a solar multiple of 2.7. Thus, assuming a yearly average hydrogen production level of 100 TPD (578 mol/s), the maximum H_2 production level during a year (i.e. average production achieved during summer solstice day) is 133.3 TPD (770 mol/s) for the 2015 scenario and 131.6 TPD (764 mol/s) for the 2025 scenario and, based upon these values, the overall HyS solar plant (HyS plant and solar plant) has been designed and cost evaluated.

As a consequence, with reference to the current flowsheet, the HyS plant power requirements for the 2015 scenario at the design point of 100 TPD are:

1. Thermal power: 333.6 MWt. The high temperature H_2SO_4 dissociation requires 275.6 MWt (which represents almost 83% of the total thermal power), while the low temperature requirement for the column boiler is 58 MWt (which represents approximately 17% of the total thermal power);
2. Electric power: 92 MWe. The SDE requires 89.2 MWe, which represents almost 97% of the total electric thermochemical plant requirement, while 2.8 MWe are needed for the HyS plant auxiliaries.

For the 2015 scenario, two solar towers are needed to drive the HyS plant, each of which delivers to the thermochemical process half the overall thermal power (i.e. approximately 167 MWt) by means of the IHX loop. Results of the ASPEN Plus® simulation of the IHX loop are reported in Table 2, with reference to the scheme in Fig. 10.

A helium flow rate of 48.3 kg/s is needed to deliver the required thermal power for each tower of the HyS plant. Helium recirculation compression power is approximately 5.4% of the HyS plant total electric power (2.5 MWe per each IXH loop) and solar thermal power absorbed by each solar receiver is approximately 164.5 MWt. Thus, given the solar multiple of 2.7, each solar tower needs sizing for the peak power of 444 MWt.

Table 2 – IHX loop (per each tower) stream table for a yearly average H_2 production rate of 100 TPD under solar operating conditions.

Stream ID	Flow rate (kg/s)	Pressure (bar)	Temperature (°C)
1 (He)	48.3	40.0	294
2 (He)	48.3	39.5	950
3 (Sand)	320.0	1.0	1000
4 (Sand)	320.0	1.0	600
5 (He)	48.3	39.0	400
6 (He)	48.3	38.7	284

Further 4.8% of the HyS plant electric power (2.25 MWe per each solar plant) is needed for solar auxiliaries (e.g. bucket lift, etc).

The 2025 scenario sees the removal of the IHX loop with the HyS plant interfaced equipment located inside the solar tower and directly heated by the falling sand particles.

For this scenario, based upon foreseen improvements about the most challenging equipment and about flowsheeting arrangement, the thermochemical plant efficiency has reasonably been assumed to achieve a value of 40% (LHV). The electric power needed to the SDE can be reasonably assumed to be 101.3 kJe/molSO_2 based upon current evaluations at SRNL about foreseen improvements. Thus the estimated thermal power needed to the HyS plant at the design point is approximately 78% of the 2015 year correspondent power (260 MWt), directly supplied by a single high temperature solar tower, without the need for the IHX loop. New equipment concepts (e.g. a new H_2SO_4 decomposition reactor directly heated inside the solar receiver, different solar HyS plant arrangements and layouts, etc.) are going to be developed and conceptually designed in the next years, aimed at removing the IHX.

To deliver to the HyS plant the (continuous) needed thermal power at the design point, the solar plant needs sizing to reach a solar peak power of approximately 700 MWt given the solar multiple of 2.7, with a reduction of more than 21% compared to the 2015 year value.

In Table 3 the annual solar plant performance is summarized for both scenarios. Thermal and electric HyS plant requirements are shown giving the values at the design point for a H_2 production rate of 133.3 TPD (131.6 TPD for the 2025 year) and the average quantities throughout the year. The needed electric power has been assumed to be taken from the grid, produced by renewable energy sources. Of course, a second solar electric plant could be coupled with the HyS plant to provide the electricity if desired, but analysis of this design was outside of the scope of the present study.

5. Plant design and economic analysis results

5.1. *Plant design*

The HyS plant has been designed and cost evaluated assuming it constituted by the following parts:

Table 3 – Annual solar plant performance for a yearly average H_2 production of 100 TPD, under solar operating conditions, for the 2015 and 2025 scenarios.

Period of the year		Peak solar power (MWt)	Total solar energy (MWht)	AVG solar power (MWt)	H_2 production (TPD)	Electricity (MWe)
Summer solstice day (24 h)	2015 yr	890	7.89 E + 3	329	133.3	101.5
	2025 yr	700	6.25 E + 3	260	131.6	84.7
All the year (8760 h)	2015 yr	890	2.15 E + 6	247	100.0 (AVG)	76.1 (AVG)
	2025 yr	700	1.71 E + 6	195	100.0 (AVG)	64.4 (AVG)

1. Electrolysis section, which comprises: (i) the SDE; and (ii) the balance of the electrolysis section equipment (anolyte coolers, recirculation pumps, etc);
2. Sulfuric acid decomposition section, which includes: (i) the H_2SO_4 bayonet reactor; and (ii) balance of the H_2SO_4 decomposition section equipment (i.e. H_2SO_4 concentration, SO_2 recirculation, SO_2–O_2 separation, etc.);
3. Feed and utility supply section.

The most challenging components are the SDE and the bayonet reactor.

The SDE module has been designed on the basis of current experimental results obtained at SRNL. The component consists of a stack of electrochemical cells configured in a hybrid bipolar arrangement utilizing proton exchange membrane (PEM) electrolytes. Each individual cell consists of a membrane electrode assembly (MEA) held between two porous carbon gas diffusion layers. Non-porous graphite bipolar plates separate cells from each other and provide flow fields for both the acid mixture and the hydrogen. Up to 200 cells are connected in series in an SDE module and constrained between steel end plates using tie rods. Gaskets between cells provide sealing for operating pressures up to 21 bar. The single module is characterized by the following features: (1) anolyte inlet flow rate of 322.3 kg/h, (2) catholyte inlet water flow rate of 56.0 kg/h, (3) voltage of 120 V (DC), (4) current of 5000 A and (5) hydrogen flow rate of 37.62 kg/h. In order to contain the required 21 bar of pressure, a circular bipolar plate cell design is adopted. Each cell has an active area of 1.0 m^2. The bipolar plates have an outer diameter of 1.22 m. The total thickness of each cell is about 0.01 m and the overall length of the 200 cell stack is approximately 2.54 m (100 inches). Each module length, including the end plates and other structural components, is approximately 3.5 m. A schematic of the single SDE module is reported in Fig. 11.

To reach the solar H_2 production rate of 133 TPD, 155 SDE modules are required (considering a 5% surplus capacity accounting for performance losses, maintenance, etc).

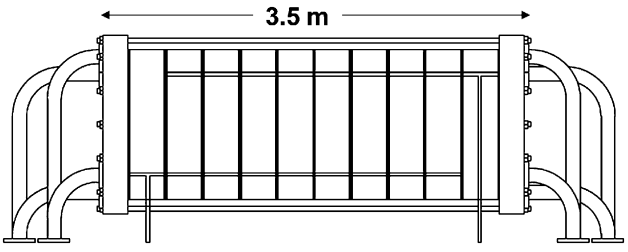

Fig. 11 – 200 cell SDE module developed at SRNL.

Platinum has been chosen as the anode and cathode catalyst material due to its good performance and excellent stability [16]. Nafion is the current baseline material for the membrane and bipolar plates are made of graphite [17].

Regarding the H_2SO_4 decomposition reactor, the bayonet features and performance are currently being investigated and improved at SNL [11]. A similar concept has also been investigated and is under development at Westinghouse Corporation [18,19]. Bayonet tubes are made of SiC material, with minimal thicknesses since both helium and HyS mixtures are at the same pressure of 40 bar under the present solar working conditions. Supported platinum has been selected as the current baseline material for catalyst although research activities are being carried out to investigate performance of other potential catalysts and to find the best solution under different operating conditions. Idaho National Laboratory (INL) has performed research under the NHI program to search for adequate catalysts for the H_2SO_4 decomposition [20,21].

The 2015 scenario configuration sees the adoption of two bayonet reactor units, each constituted of approximately 950 tubes in parallel, located close to the two solar towers and heated by the solar IHX fluid, with the remainder of the HyS plant equipment located in a single area. The 2025 scenario sees a single bayonet reactor, constituted of almost 2000 tubes, inside the solar tower and directly heated by the hot falling sand particles.

The remainder of the HyS plant (i.e. more traditional equipment) has been designed considering traditional engineering rules and relationships applied to components which work under aggressive operating conditions. Traditional shell and tube heat exchangers have been adopted as heat transfer devices made of massive metallic materials (both tube side and shell side) for the different HyS plant sections. Depending on the specific environment some shell units have been assumed made of carbon steel material, coated with more expensive metal materials. Cold water has been assumed as the cold utility fluid to remove low temperature heat from the HyS process. Knock out equipment has been sized considering massive metallic material for shells, capable to resist aggressive conditions. Vacuum tower and SO_2 absorber shells have been assumed made of massive metallic materials, while ceramic packing trays have been adopted for both towers. Pumps and SO_2 recycle compressor have been designed following traditional rules, with metallic constitutive materials. The conceptual design of the HyS process was modified from that developed in conjunction with a major engineering firm based on a nuclear driven HyS cycle. More details about equipment design for the nuclear case will be released in another publication.

The solar plant, likewise the thermochemical plant, can be assumed constituted by the following sections:

1. Heliostat field
2. Tower receivers
3. Piping and Towers
4. Thermal storage tanks
5. Controls
6. Balance of plant

The solar plant has been designed jointly with SNL taking into account their data and quantities [22]. For the 2015 scenario, each of the two solar plants requires approximately a heliostat field area (mirror area) of 858,000 m^2, to reach a single solar receiver thermal peak power of about 444 MWt. Regarding the 2025 scenario, the single tower is fed by a solar field which extends over a mirror area of approximately 1,400,000 m^2 to reach the peak power of about 700 MWt. SNL's DELSOL program has been used to predict the tower height, which results in 230 m (340 m for the 2025 year).

Each tower thermal storage tanks need sizing for a maximum capacity of approximately 2200 MWh (13 h of storage at the AVG solar power during the summer solstice day), for the 2015 year, while for the 2025 year the single tower tanks need sizing for a capacity of approximately 3400 MWh. With sand features available from [23] each tank needs sizing to contain a volume of approximately 4000 m^3 (7000 m^3 for the 2025 scenario).

Regarding the IHX loop, the selection of the best IHX device (i.e. the best technology in terms of capital investment, lifetime costs and reliability of the component) is currently under investigation at SRNL. Presently the cross counter current heat exchanger concept has been selected as the baseline approach (Fig. 12) and a preliminary design has been achieved with the aim of finding an indicative heat transfer area, to evaluate the cost of the device. With reference to Fig. 12, hot sand vertically falls in the device (from 1000 °C to 600 °C), while helium goes inside tubes to the top of the device (from 294 °C to 950 °C) in a cross counter current arrangement.

SiC has been assumed as the constitutive tube material, based upon considerations and choices currently carried out for nuclear IHX's and its excellent thermal conductivity features.

Thermal power exchanged between sand and helium can be expressed by the classical relationship (6):

$$W = U_g \cdot S \cdot \mathrm{LMTD} \cdot f \tag{6}$$

The corrected LMTD is about 120 °C (assuming an f value of 0.85 from Ref. [24]).

Neglecting conductive phenomena (since SiC shows high thermal conductivity) the overall heat transfer coefficient (U_g) can be estimated according to the following formula:

$$1/U_g = 1/U_H + 1/U_S \tag{7}$$

To evaluate U_H, Dittus and Boelter correlation has been adopted:

$$\mathrm{Nu_H} = 0.023 \mathrm{Re_H^{0.8}} \mathrm{Pr_H^{0.3}} \tag{8}$$

Fixing the maximum pressure drops inside tubes at 0.5 bar, with $\mathrm{Re_H}$ equal to about 95,000 and a helium volumetric flow rate of 261 m^3/h (0.073 m^3/s) (per tube), U_H is approximately 1350 W/m^2 K.

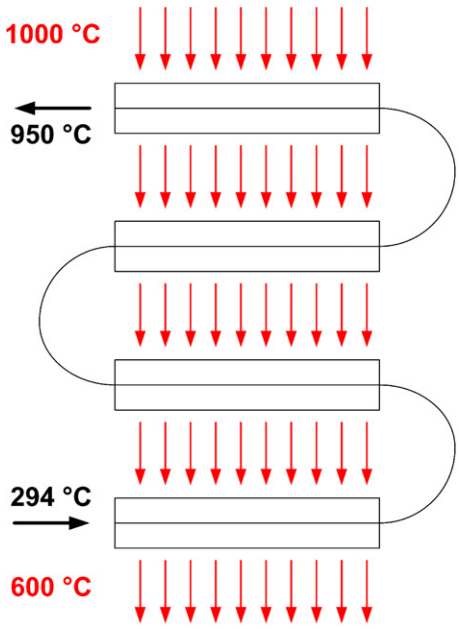

Fig. 12 – Cross counter current-based IHX model: sand goes vertically down (from 1000 °C to 600 °C) and helium goes up inside tubes (from 294 °C to 950 °C) in a cross counter current arrangement.

Regarding the U_S coefficient, for shell (i.e. sand) side, Kurochkin's formula [25] has been adopted with particles impacting circular tubes:

$$\mathrm{Nu_S} = 0.0214\, \mathrm{Pe_S^{0.21}} (D_T/d_p) \tag{9}$$

With features available from Ref. [23], an average particle diameter of 600 μm and a tube diameter of 0.05 m, U_S has been estimated in approximately 1625 W/m^2 K. Thus, the overall Sand–Helium heat transfer coefficient is approximately 740 W/m^2 K and an area of 1850 m^2 is needed to exchange 164.5 MWt between hot sand and helium, for each IHX.

5.2. *Economic analysis*

5.2.1. *Methodology and assumptions*

Hydrogen production cost has been assessed considering the H2A economic rules and guidelines and assuming US $ of the year 2005 for both scenarios as the baseline currency.

To evaluate the capital investment cost, a specific heliostat cost of 126.5 $/$m^2$ has been assumed for the 2015 scenario and 90 $/$m^2$ for the 2025 year [26]. Solar receiver direct costs have been assessed scaling up values available from Ref. [27] as well as towers and piping costs have been estimated on the basis of the cost algorithm available from Ref. [27]. Thermal storage costs have been evaluated assuming a specific cost of 500 $/ton for alumina sand and an installed cost of 8 $/kWh (7 $/kWh for the 2025 year) for the tanks on the basis of Ref. [22]. Costs of controls and balance of solar plant equipment have been taken from Ref. [27] and suitably modified and adapted to the current plant.

Regarding the thermochemical process, the SDE costs have been calculated on the basis of economic considerations

carried out at SRNL resulting in a specific (not installed) cost of 273.6 k$ per module (or 456 $/kWe) for the 2015 scenario. More than 72% of SDE module uninstalled cost is due to SDE cells which constitute the module, with the remainder constituted by end plates, tie rods, collectors, piping connections, module supports, module assembly and installation working cost, etc. The single cell cost is mainly due to catalysts (approximately 40%) and membrane (approximately 24%), while the remainder is substantially due to carbon diffusion layers (about 12%) and graphite bipolar plates (approximately 16%). Based on current evaluations being carried out at SRNL a SDE specific cost of 300 $/kWhe has been selected for the long term scenario according to foreseen cost improvements. An installation factor of 1.2 (which is a typical value for electrolyzers) has been adopted to evaluate the SDE installed cost. Concerning the bayonet reactor, costs coming from nuclear case economic evaluations (carried out along with Westinghouse Electric Co.) have been suitably adapted and scaled to the solar application adopting a scaling down (exponential) cost factor of 0.55, on the basis of information provided by TIAX, LLC. An uninstalled cost of approximately 17 M$ has been assessed for the 133 TPD solar rate hydrogen production. The major part of this cost is due to bayonet tubes (69%), catalyst (approximately 9%) and vessel head (almost 8%). An installation factor of 1.44 has been assumed on the basis of considerations carried out along with an engineering firm partner. As a consequence, the bayonet installed cost has been estimated in 24 M$ for the solar H_2 production rate of 133 TPD.

Costs of the other (more traditional) equipment (i.e. balance of the electrolysis section, balance of the H_2SO_4 section and feed and utility) of the HyS plant have been evaluated using the Aspen K-Base software and suitably revising those already calculated for the nuclear case. IHX loop preliminary cost evaluations have been carried out adapting available cost databases already adopted to assess costs of nuclear and solar driven thermochemical processes [28,29]. Values so obtained have been compared to costs assessed for nuclear H_2 production plants and a good agreement has been noticed. The IHX loop piping cost evaluations have been carried out suitably scaling values already obtained for nuclear applications [30].

Indirect costs included: (1) site preparation costs, (2) engineering and design costs, and (3) up front owner's cost. Site preparation costs have been evaluated based upon information reported at table E-2 in Ref. [27] and so resulting in 1.3 (1.5 for the 2025 case) the cost of land. Engineering and design costs have been assumed equal to 17.7% of solar plant costs [27] and 3% of the thermochemical plant costs, based on evaluations carried out at SRNL[3]. Owner's costs have been evaluated as 3% of direct costs based on previous evaluations carried out on nuclear driven thermochemical plants. An overall project contingency equal to 16.6% of solar plant direct cost [27] plus 15% of the thermochemical plant cost (on the basis of nuclear case assessment) have been added to evaluate total indirect costs.

[3] The majority of the engineering and design costs for the HyS plant were already included in the installed costs of the equipment.

Table 4 – HyS solar plant investment costs.

	Beginning construction Year 2015	Beginning construction Year 2025
DIRECT COSTS [US 2005 M$]		
Solar plant costs		
Heliostat (M$)	217.3	125.7
Receiver (M$)	16.9	10.1
Tower and piping (M$)	24.0	29.0
Storage (M$)	31.4	23.3
Control systems (M$)	1.6	1.6
Balance of plant (M$)	21.4	18.3
Subtotal – Solar plant (M$)	**312.6**	**208.0**
HyS plant costs		
H_2SO_4 decomposition and balance (M$)	79.7	82.4
Electrolysis and balance of electrolysis (M$)	52.5	31.7
Feed and utility supply (M$)	6.1	6.1
Subtotal – HyS plant (M$)	**138.3**	**120.2**
IHX costs (40 bar case) (for the two towers)		
IHX (M$)	8.0	–
Circulation compressor (M$)	4.0	–
Piping (M$)	3.6	–
Subtotal – IHX loop (M$)	**15.6**	–
TOTAL INSTALLED COSTS (M$)	**466.5**	**328.2**
INDIRECT COSTS [US 2005 M$]		
Site preparation (M$)	6.8	5.4
Engineering (M$)	59.5	40.4
Owner's costs (M$)	14	9.9
Project contingency (M$)	73.1	52.6
TOTAL INSTALLED + INDIRECT COSTS (M$)	**620**	**436.5**
INVESTMENT COSTS [US 2005 M$]		
Land (M$)	5.2	3.7
TOTAL INVESTMENT COST (M$)	**625.1**	**440.2**

HyS solar plant investment costs (subtotal costs are in bold text).

HyS solar plant lifetime costs have been estimated following the H2A guidelines for fixed O&M costs. Electricity needed to sustain the overall process has been assumed to be purchased at 6.8 c$/kWh for the 2015 scenario and 4.8 c$/KWh for the 2025 scenario, produced by solar power plants.

The replacement of the SDE (complete replacement) and bayonet reactor (tubes) have been foreseen every 5 years (10 years for the long term scenario) and suitably cost accounted and integrated in the cost breakdown. Decommissioning of the overall plant has also been included in the cost evaluations.

Financing H2A guidelines have also been assumed to assess the final H_2 production specific cost. In particular, the plant lifetime has been fixed equal to 40 years, depreciation length equal to 20 years (with MACRS method) and taxes have been assumed equal to 38.9% with a real IRR of 10% and an

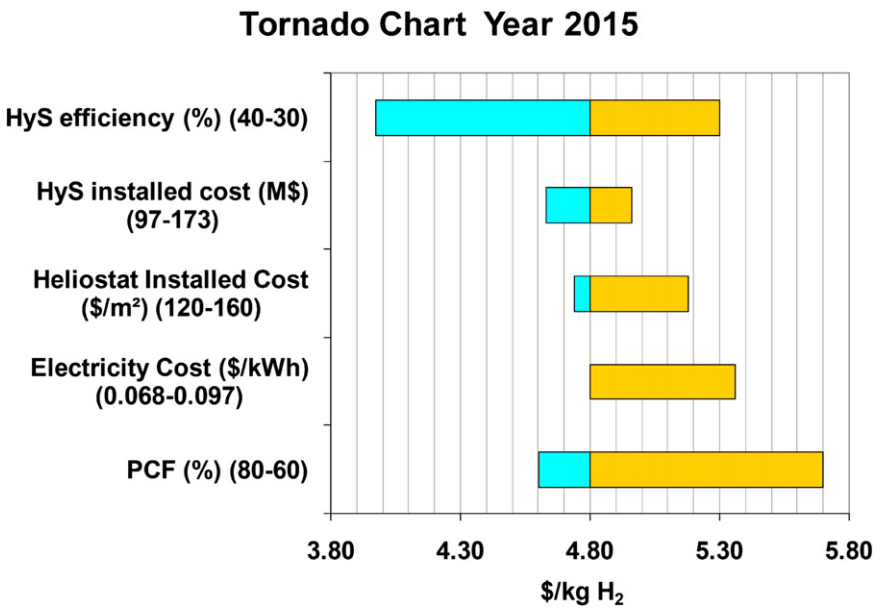

Fig. 13 – Specific H_2 production cost sensitivity analysis (Tornado Chart) for the 2015 year, varying the HyS plant efficiency (the baseline value is 33%), the HyS installed costs (the baseline value is 138.3 M$), the heliostat installed costs (the baseline value is 126.5 $/m^2), the electricity cost (the baseline value is 0.068 $/kWh) and the PCF (the baseline value is 75%).

inflation rate of 1.9%. The plant construction time length has been assumed equal to 3 years.

5.2.2. *Cost results*

Capital investment cost results are shown in Table 4, for both scenarios.

The overall solar HyS plant direct installed costs represent approximately 75% of the total investment costs for both scenarios, while indirect costs and land represent the remaining 25%. The total investment cost for the Year 2015 plant is $625 million, whereas the cost is reduced to $440 million for the Year 2025 design. The solar plant represents 67% of the direct costs for the Year 2015 plant, while the HyS plant represents 30% and the IHX loop 3%. For the Year 2025 design, these ratios are 63%, 37% and 0%, respectively. For the 2015 scenario approximately 70% of the solar plant costs is constituted by the heliostat field cost, which reaches 47% of the overall plant installed costs. For the 2025 scenario the heliostat field cost is only 60% of the solar plant cost, representing 38% of the total installed cost. The remainder of solar plant costs is due to the receiver costs (approximately 5% for both the 2015 and 2025 year), the tower and piping costs (almost 8% for the 2015 year and 14% for the 2025 year), the storage system costs (approximately 10% for the 2015 and 11% for the 2025 year) and the balance of plant costs (almost 7% for the 2015 and approximately 9% for the 2025 year).

Table 5 – HyS solar plant lifetime costs.

	Beginning construction Year 2015	Beginning construction Year 2025
FIXED O&M COSTS [US 2005 M$/y]		
Labor (M$/y)	3.1	2.3
G&A (M$/y)	0.6	0.5
Property taxes and insurance (M$/y)	8.3	6.0
Material for maintenance and repairs (M$/y)	9.2	8.3
TOTAL O&M FIXED COST (M$/y)	**21.3**	**17.1**
VARIABLE O&M COSTS [US 2005 M$/y]		
Demineral water (M$/y)	0.4	0.4
Purchased Electricity (M$/y)	45.4	27.1
TOTAL VARIABLE O&M COST (M$/y)	**45.8**	**27.5**

HyS solar plant lifetime costs (subtotal lifetime costs are in bold text).

The HyS plant is responsible for 30% (almost 37% for the 2025 scenario) of the overall installed costs. Approximately 38% (more than 26% for the 2025 scenario) of the thermochemical plant costs is due to the electrolysis section while the H_2SO_4 decomposition section contributes for more than 58% (more than 68% for the 2025 scenario[4]) and the remainder (4% for the 2015 scenario and approximately 5% for the 2025 year) is represented by the feed and utility supply section installed costs. In particular the contribution of the two most distinguishing components of the thermochemical plant is detailed in the following. The SDE installed cost represents approximately 79% (73% for the 2025 scenario) of the overall cost of the electrolysis section, resulting in 30% (approximately 19% for the long term scenario) of the thermochemical

[4] The 2025 scenario percent includes the matching system between the H_2SO_4 decomposition bayonet reactor (located inside the solar tower) and the remainder of the HyS plant (on the ground), which cost results in approximately 15% of the H_2SO_4 decomposition reactor cost.

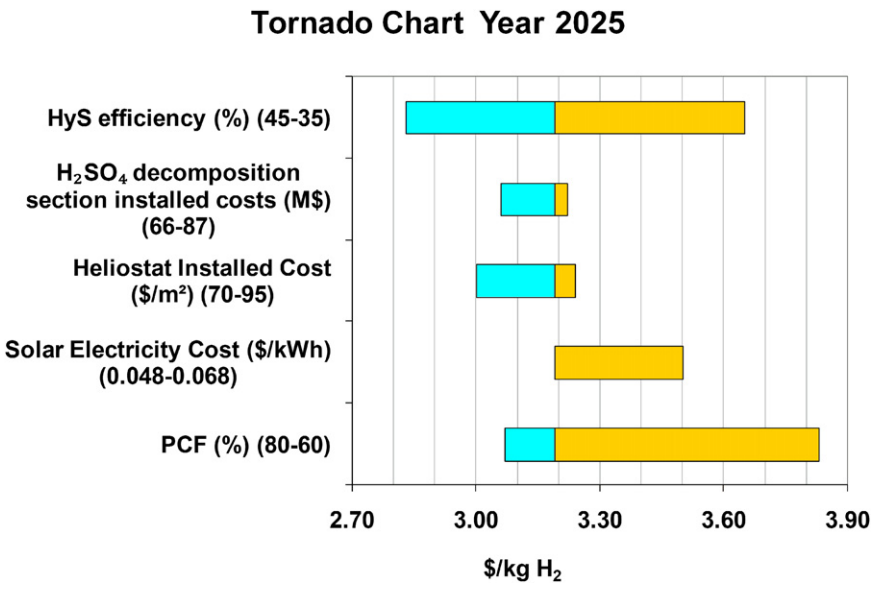

Fig. 14 – Specific H_2 production cost sensitivity analysis (Tornado Chart) for the 2025 year, varying the HyS plant efficiency (the baseline value is 40%), the H_2SO_4 decomposition section installed costs (the baseline value is 82.4 M$), the heliostat installed costs (the baseline value is 90 $/m^2), the electricity cost (the baseline value is 0.048 $/kWh) and the PCF (the baseline value is 76%).

plant installed costs. The bayonet installed cost is approximately 30% (29% for the 2025 year) of the H_2SO_4 decomposition section costs affecting the HyS plant cost for more than 17% (20% for the longer scenario). As a consequence, it is important to note that the balance of the H_2SO_4 decomposition section strongly influences the overall thermochemical plant installed costs, resulting in approximately 40% (almost 49% for the long term scenario).

This highlights that the influence of the SDE on the installed cost of the HyS plant is less than 30% and is lower than that of the balance of the sulfuric acid decomposition section.

The IHX loop, for the 2015 scenario, contributes on the solar HyS plant installed costs for approximately 3%.

Indirect costs, which affect the total investment cost for approximately 24% for both scenarios, are constituted for approximately 47.5% (48.5% for the long term period) by contingencies, which are the most important item, and for approximately 39% (37% for the 2025 scenario) by engineering and design costs. The remainder is due to site preparation (4.5% for the 2015 year and 5% for the 2025 year) and owner's costs (9% for both scenarios).

In Table 5 plant lifetime costs are reported. For the 2015 scenario, almost 68% of the overall lifetime costs is due to electricity cost (which represents 99% of the variable O&M costs for both scenarios), while for the 2025 year, with the thermochemical plant efficiency equal to 40% and the electricity cost equal to 4.8 c$/kWh, the electric consumption represents approximately 38.5% of the overall cost. Regarding fixed O&M costs, the most relevant item is due to maintenance and repairs material which influences fixed O&M costs for more than 43% for 2015 year and more than 48% for long term scenario. Taxes and insurance affect fixed O&M costs for almost 39% (2015 scenario) and 35% (2025 year). The remainder of the fixed O&M costs is basically represented by labor costs.

Following rules and financing H2A guidelines, a hydrogen production cost of 4.80 $/kg has been assessed for the 2015 year and 3.19 $/kg for the 2025 scenario. Capital investment-related cost influences the H_2 specific (i.e. per kg of H_2) cost for 61% for both scenarios. Approximately 13% (15% for the long term) of the H_2 specific cost is due to fixed O&M and the remainder (26% for the 2015 year and 24% for the 2025 year) is constituted by variable O&M specific costs, almost entirely due to electric power cost. Decommissioning influence is less than 1% on the total H_2 production cost.

5.2.3. *Sensitivity analysis*

Specific H_2 production cost sensitivity analyses have been carried out, varying the most cost influencing parameters and assumptions as shown in Fig. 13 and Fig. 14. The H_2 production cost is strongly affected by the HyS plant efficiency for both scenarios, since both the specific investment cost of the solar plant and the specific electric consumption are strongly influenced by the thermochemical plant efficiency. A first sensitivity analysis has been performed to evaluate the influence of the efficiency on the cost without re-designing ex novo the HyS plant but, basically, assuming a lower (or higher) H_2 production level of the plant corresponding to a lower (or higher) efficiency[5]. An increase of 21% of the efficiency for the 2015 scenario (passing from 0.33 to 0.4) results in an important reduction of the H_2 specific cost of more than 17% with a specific cost lower than 4 $/kg, while a reduction of the efficiency of 9% (from 0.33 down to 0.3) implies an increase of the production cost of approximately 10%. Likewise for the long term scenario, an increase of the efficiency of 12.5% (from

[5] A re-design of the thermochemical plant would be needed to evaluate more precisely how the efficiency affects the HyS plant installed cost.

0.4 to 0.45) results in a specific cost lower than 2.85 $/kg, with a reduction of approximately 11%.

A second sensitivity analysis has been carried out seeing the influence of the investment cost variation on the H_2 production cost, starting from the heliostat field which represents the most important investment cost item. For the 2015 scenario, a rise of almost 26% (from 127 $/m^2 to 160 $/m^2) results in a H_2 production cost increase of approximately 8%, up to 5.20 $/kg. An augmented heliostat cost of approximately 5.5% (from 90 $/m^2 to 95 $/m^2) for the 2025 year results in a specific H_2 cost of 3.24 $/kg (almost 2% higher than the baseline cost). Regarding the HyS plant costs, the analysis has been carried out assuming selected and reasonable percent variation of the installed cost. Results show that a variation of the overall installed cost of the thermochemical plant of 30% (from 138.3 M$ to 97 M$) causes a variation of H_2 specific cost of approximately 4% (from 4.80 $/kg to 4.63 $/kg) for the 2015 scenario. For the longer term scenario, the influence of the H_2SO_4 decomposition section cost variation in the range of −20% (66 M$) to +5% (87 M$) has been evaluated and a maximum reduction of 4% of the H_2 production cost (from 3.19 $/kg to 3.06 $/kg) has been assessed. The HyS plant installed costs can be reduced not only lowering the cost of the SDE and the bayonet reactor, but also considering different materials (e.g. internal lining, ceramic materials, etc.) and technologies (e.g. different heat transfer devices) for the balance of the H_2SO_4 decomposition section equipment, resulting in important H_2 cost decreases especially for the 2025 scenario. Concerning lifetime cost, the electricity price is the assumption which most affects the production cost. An increase of 3 cents/kWh leads to a H_2 cost increase of 12% for the 2015 year, with a value higher than 5.3 $/kg, while, for the 2025 year, an increase of 2 cents/kWh implies an H_2 specific cost of approximately 3.50 $/kg (almost 10% higher than the baseline value for the long term).

Finally a variation of the PCF in the range of 0.6–0.8 has been considered for both scenarios, accounting for uncertainties in the solar plant efficiency and annual insulation. The PCF variation affects the hydrogen production level and, in turn the efficiency of the plant. Results, reported at Fig. 13 and Fig. 14, show that with a PCF of 60% the H_2 production cost increases of about 19%, while a PCF of 80% leads to a specific cost reduction of approximately 4% for both scenarios.

All the economic evaluations and assumptions have also been validated by TIAX Company as part of the work carried out in the DOE STCH project, to ensure consistency with other hydrogen production options under consideration.

6. Summary and conclusions

Conceptual design and economic analysis of a solar H_2 production plant based on the HyS thermochemical process, matched to a particle receiver-based solar tower, have been carried out for a large scale hydrogen production plant (100 TPD).

The most challenging components of the HyS plant are the SDE and the H_2SO_4 decomposition reactor.

SRNL is deeply involved in the study, development and construction of the SDE, both for nuclear and solar driven thermochemical processes. A cell voltage of −0.6 V, with a current density of 500 mA/m^2, seems to be an attainable value to react SO_2 dissolved in a H_2SO_4–H_2O mixture at 50 wt.%, at 21 bar and 100 °C and such values have been taken as the baseline quantities for the present analysis.

The bayonet-based reactor concept has been selected to decompose H_2SO_4 into SO_2 at high temperature. Presently SNL is the main developer partner of this component, for nuclear and solar driven thermochemical sulfur-based processes. Pinch analysis of the bayonet has been carried out at SRNL and results obtained from an ASPEN Plus® simulation for solar case operating conditions (i.e. maximum temperature of 920 °C, pressure of 40 bar and inlet H_2SO_4 water mixture concentration of 75 wt.%) have been shown in the paper and used as the basis to evaluate the high temperature external thermal power to be delivered to the HyS process.

A new HyS cycle chemical flowsheet has been set up and simulated at SRNL considering only proven commercial equipment for (more) traditional sections of the thermochemical process, aiming at achieving the highest possible efficiency and the best integration between the SDE and the Bayonet reactor.

To combine the SDE and the bayonet reactor, the H_2SO_4 mixture produced by the SDE needs to be concentrated up to 75 wt.%. The H_2SO_4 mixture concentration has been realized by two flashes in series, followed by a vacuum column, which requires low temperature external thermal power for the reboiler. Both high temperature and low temperature external thermal powers have been assumed to be supplied by the same solar tower plant.

Further activities are in progress to improve SDE and bayonet reactor performances, also considering different working conditions (e.g. different acid concentrations, temperatures, pressures), which might require continuous updating of the reference HyS flowsheet to reach the best integration between the two components.

A new matching concept between the thermochemical and the solar plants based on the sand particle solar receiver has been set up, accounting for thermal storage issues too. To deliver the needed thermal power to the chemical plant an IHX loop has been introduced, allowing for potential leverages from nuclear applications. A preliminary design of the system has also been shown in the paper. However, further R&D activities are required to reach the ultimate (i.e. economic, efficient and reliable) design of the IHX loop system. This implies that the overall solar HyS plant could be updated depending on the IHX loop choice and design, requiring modifications of flowsheet, process design, etc.

Solar HyS plant conceptual design has been presented in the paper. Ad hoc considerations have been carried out to design the SDE, the bayonet and more traditional solar plant equipment. The heliostat field and the solar tower have been designed in conjunction with SNL, on the basis of their suggestions and evaluations.

To carry out the economic analysis of the solar HyS plant, the DOE H2A analysis guidelines have been assumed, considering two different time scenarios. The first one sees the 2015 as the starting year, while the second one, for a longer period, sees the starting year at 2025. Suitable evaluations have been carried out with particular attention on the most important equipment of the plant (SDE, bayonet reactor, IHX loop, heliostat field, etc.) and reasonable assumptions made to

evaluate both investment and plant lifetime costs. An H_2 specific cost of 4.80 $/kg (2005 US $) has been estimated for the 2015 scenario. A strong cost reduction, down to 3.19 $/kg, has been found out in the longer term period, basically accounting for: (1) lower cost of heliostat field, (2) lower cost of the electrolysis section, based upon improvements and "learning" foreseen at SRNL, and (3) improvements in the overall flowsheet and layout of the HyS solar plant (e.g. increased efficiency of the thermochemical process up to 40%, removal of the IHX loop with direct heating of the H_2SO_4 decomposer, etc.). Moreover, sensitivity analyses have been carried out to show the influence of selected quantities and assumptions on the specific H_2 production cost, which has reached values lower than 4 $/kg for the 2015 year and approximately equal to 2.85 $/kg for the 2025 scenario.

Both the SDE and the bayonet device have been tested successfully at SRNL and SNL respectively, for productions up to 300 l/h. On the basis of results achieved and on experimental outcomes, it can be stated that the HyS plant is an attractive process to produce H_2 using solar energy.

Acknowledgments

This work was performed as part of the DOE Solar Thermochemical Hydrogen (STCH) project. Dr. Richard Farmer is the DOE technology manager and his help and direction have been appreciated. Interactions and useful suggestions came from Dr. Gregory J. Kolb and Dr. Nathan P. Siegel (both SNL) and Dr. Kurt Roth (TIAX), regarding the solar field design and revision of cost evaluations. The authors wish to thank Dr. Maximilian Gorensek (SRNL) for his useful suggestions.

REFERENCES

[1] Iwasaki W. A consideration of the economic efficiency of hydrogen production from biomass. Int J Hydrogen Energy 2003;28(9):939–44.
[2] Ivy J. Summary of Electrolytic hydrogen production. Milestone Report. NREL/MP-560–36734; 2004.
[3] Brown LC, Besenbruch GE, Lentsch RD, Schultz KR, Funk JF, Pickard PS, et al. High efficiency generation of hydrogen fuels using nuclear power. Final Technical Report from General Atomics Corp. to US DOE. GA-A24285; 2003.
[4] Funk JE. Thermochemical hydrogen production: past and present. Int J Hydrogen Energy 2001;26(3):185–90.
[5] Gorensek MB, Summers WA. Hybrid Sulfur flowsheets using PEM electrolysis and a bayonet decomposition reactor. Int J Hydrogen Energy 2009;34(9):4097–114.
[6] Beghi GE. A decade of research on thermochemical hydrogen at the joint research centre. Ispra Int J Hydrogen Energy 1986; 11(12):761–71.
[7] Brecher LE, Wu CK. Electrolytic decomposition of water. Westinghouse Electric Corp., US Patent No. 3888750, 1975.
[8] Farbman GH. The conceptual design of an integrated nuclear-hydrogen production plant using the sulfur cycle water decomposition system. NASA Contr. Report, NASA-CR-134976; 1976.
[9] Brecher LE, Spewock S, Warde CJ. The Westinghouse Sulfur Cycle for the thermochemical decomposition of water. Int J Hydrogen Energy 1977;2(1):7–15.
[10] Lu PWT, Ammon RL, Parker GH. A study on the electrolysis of sulfur dioxide and water for the sulfur cycle hydrogen production process. NASA Contr. Report, NASA-CR-163517; 1980.
[11] Parma EJ, Vernon ME, Gelbard F, Moore RC, Stone HBJ, Pickard PS. Modeling the sulfuric acid decomposition section for hydrogen production. In: Proceedings of 2007 int topical meeting on safety and techn. of nucl hydrogen production. Boston: Control and Mgmt; June 24–28, 2007. p. 154–60.
[12] Falcone PK, Norig JE, Hruby JM. Assessment of a solid particle receiver for a high temperature solar central receiver system. Sandia Report, SAND85–8208; 1985.
[13] Falcone PK. A handbook for solar central receiver design. Sandia Report, SAND86–8009; 1986.
[14] Kolb GJ, Diver RB, Siegel NP. Central-Station solar hydrogen power plant. J Solar Energy Eng 2007;129:179–83.
[15] U.S. Department of Energy. DOE H2A analysis database. http://www.hydrogen.energy.gov/h2a_analysis.html; 2008.
[16] Colon-Mercado HR, Hobbs DT. Catalyst evaluation for a sulfur dioxide-depolarized electrolyzer. Electrochemistry Communications 2007;9:2649–53.
[17] Summers WA, Steimke JL, Hobbs DT, Colon-Mercado HR, Gorensek MB. Development of a sulfur dioxide depolarized electrolyzer for the Hybrid Sulfur thermochemical process. High temperature reactor Conference 2008, Washington, USA, September 30, 2008.
[18] Connolly SM, McLaughlin DF, Lahoda EJ. Design of composite sulfuric acid decomposition reactor, concentrator and preheater for hydrogen generation processes. Int J Hydrogen Energy 2009;34(9):4074–87.
[19] Connolly SM, Lahoda EJ, McLaughlin DF. Processes, design of recuperative sulfuric acid decomposition reactor for hydrogen generation. Philadelphia, USA. In: Proceedings of AIChE 2008 annual meeting; 2008.
[20] Ginosar DM, Glenn AW, Petkovic LM, Burch KC. Stability of supported platinum sulfuric acid decomposition catalysts for use in thermochemical water splitting cycles. Int J Hydrogen Energy 2007;32(4):482–8.
[21] Ginosar DM, Rollins HW, Petkovic LM, Burch KC, Rush MJ. High-temperature sulfuric acid decomposition over complex metal oxide catalysts. Int J Hydrogen Energy 2009;34(9):4065–73.
[22] Kolb GJ. Personal communication; 2008.
[23] Chen H, Chen Y, Hsieh H-T, Siegel NP. Computational fluid dynamics modeling of gas particle flow within a solid particle solar receiver. J Solar Energy Eng 2007;129:160–9.
[24] Perry RH, Green DW. Perry's chemical Engineers' Handbook. VII ed. McGraw-Hill International Editions; 1997.
[25] Kurochkin P. Heat transfer between tubes of different sections and a stream of granular material. J Eng Phys 1966; 10(6):759–63.
[26] Kolb GJ, Jones SA, Donnelly MW, Gorman D, Thomas R, Davenport R, et al. Heliostat cost reduction study. Sandia Report, SAND2007–3293; 2007.
[27] Sargent and Lundy Group Consulting. Assessment of parabolic trough and power tower solar technology cost and performance forecasts. SL-5641, 2003.
[28] Le Duigou A, Borgard JM, Larousse B, Doizi D, Allen R, Bruce EC, et al. HYTHEC: an EC funded search for a long term massive hydrogen production route using solar and nuclear technologies. Int J Hydrogen Energy 2007;32:1516–29.
[29] Cerri G, Salvini C, Corgnale C, Giovannelli A, De Lorenzo M, Martinez A, et al. Sulfur–Iodine plant for large scale hydrogen production by nuclear power. Int J Hydrogen Energy 2010;35:4002–14.
[30] Summers WA. Centralized hydrogen production from nuclear power: infrastructure analysis and test-case design study. Final Project Report, Phase B Test-Case Preconceptual Design. NERI Project 02–160, WSRC-MS-2005-00693. Westinghouse Savannah River Company, SRNL, Aiken; 2006.